

Missing Linker Defects in a Homochiral Metal Organic Framework: Tuning the Chiral Separation Capacity

Benjamin Slater^{†,§‡} Zeru Wang,^{†,§} Shanxue Jiang,[†] Matthew R. Hill,[‡] Bradley P. Ladewig^{*,†}.

[†]Barrer Centre, Department of Chemical Engineering, Imperial College London, United Kingdom

[‡]CSIRO, Private Bag 10, Clayton South MDC, Victoria 3169, Australia

KEYWORDS: *chiral separation, homochiral metal organic framework, missing linker defects, ZnBLD*

ABSTRACT: Efficient chiral separation remains a very challenging task due to the identical physical and chemical properties of the enantiomers of a molecule. Enantiomers only behave differently from each other in the presence of other chiral species. Homochiral metal organic frameworks have received much attention for their promising enantioseparation properties. However, there are still challenges to overcome in this field such as high enantiomeric separation. Structural defects play an important role in the properties of MOFs and can significantly change the pore architecture. In this work, we introduced missing linker defects into a homochiral metal organic framework [Zn₂(bdc)(L-lac)(dmf)] (ZnBLD) and observed an increase in enantiomeric excess for 1-phenylethanol of 35% with the defective frameworks. We adjusted the concentration of monocarboxylic acid ligand L-lactic acid by varying the ratio of Zn²⁺ to ligand from 0.5 to 0.85mmol. Additionally, a defective framework was synthesized with propanoic acid as modulator. In order to elucidate the correlation between defects and enantiomeric excess, five characterization techniques (FTIR, TGA, ¹H NMR, ICP and PXRD) were employed. Full width at half maximum analysis (FWHM) was performed on the powder x-ray diffraction traces and showed that the higher concentration of monocarboxylic acid MOFs were isostructural but suffered from increased FWHM values.

INTRODUCTION

Separation of racemic chemicals plays a significant role in pharmaceutical development, as a result of different pharmacological and toxicological properties of enantiomers. Because of some shortcomings such as high price and low efficiency of conventional methods (e.g., chromatography) for chiral resolution.¹ Metal organic frameworks (MOFs), a class of crystalline porous material have proven to be an excellent candidate for enantiomeric separations,² amongst other promising applications like catalysis,³ drug delivery,⁴ and gas separation,⁵ due to their high porosity and highly tunable structure. Host-guest interactions between the framework and guest molecules can vary dramatically with the changing size of guest molecules, having profound implications on the observed enantiomeric excesses. This was demonstrated with the separation of racemic methyl and ethyl lactate, where the extra carbon caused the enantiomeric excess to drop from 65.8% to 14.9%.⁶ Similarly a homochiral hydrogen bonded framework showed dramatic decreases in enantiomeric excess from 2-butanol (77%ee) to 2-heptanol (<4%ee).⁷

A promising homochiral MOF, ZnBLD [Zn₂(bdc)(L-lac)(dmf)](DMF) (bdc = 1,4-benzenedicarboxylic acid, L-

lac = L-lactic acid, dmf=N,N'-dimethylformamide) has drawn much attention for enantioselective separation of racemic mixtures, such as chiral alcohols,⁸ and alkyl aryl sulfoxides,^{3d} observing enantiomeric excess (ee%) values of up to 21% and 27%, respectively. ZnBLD is synthesized from zinc nitrate, 1,4-benzenedicarboxylate and L-lactic acid in a 1:0.5:0.5 ratio.^{2d}

Recent research has focused on defect engineering of MOFs and readers are directed to two thorough reviews on this subject.⁹ Fang et al. defined defects as “sites that locally break the regular periodic arrangement of atoms or ions of the static crystalline parent framework because of missing or dislocated atoms or ions”. Similarly, Sholl and Lively very broadly defined defects as “any deviations from an ideally ordered crystal structure”. An interesting class of defects contain missing linkers which have been appropriately named as missing linker defects.¹⁰ Modulated synthesis is the intentional addition of missing linker defects into MOFs and allows researchers to tune a MOF's properties by partially substituting multi-coordinating bridging linker ligands such as 1,4-benzenedicarboxylate with non-bridging ligands such as acetic acid.¹¹ This technique can significantly change the pore architecture and properties. Defective UiO-66 has been thoroughly investigated and defective frameworks have benefitted from higher porosity

and BET surface areas,^{11a,12} increased catalytic activity,¹³ and tunable thermomechanical properties.¹⁴

Inspired by recent work on defect engineering of metal organic frameworks, we investigated the influence missing linker defects have on the enantioseparation properties of ZnBLD. By synthesizing a series of ZnBLD MOFs with varying concentrations of monocarboxylic acid (see Scheme 1). *L*-lactic acid and propanoic acid were used as modulators. We correlate defect concentration with enantioselective capacity. All frameworks were characterized by Fourier-transform infrared spectroscopy (FTIR), powder x-ray diffraction (PXRD), Zn analysis by inductively coupled plasma (ICP), ¹H nuclear magnetic resonance (after MOF digestion) (¹H NMR) and thermogravimetric analysis (TGA) (unless otherwise stated). The separation capacity for three chiral molecules 1-phenylethanol, pantolactone and 2-butanol were determined by chiral gas chromatography (GC). Additionally, two different crystal washing methods were compared, DMF washing or DMF and Et₂O washing respectively (See Scheme S1). Samples were used without prior activation as is common with gas applications, taking advantage of the dynamic process of chiral recognition.¹⁵ There was a significant difference in the chiral separation capacity between the two washing techniques for the separation of 1-phenylethanol. By tailoring the pore architecture, our separation performance is significantly higher than the 21ee% previously reported for 1-phenylethanol.⁸ Frameworks were named based on the molar ratio of *L*-lactic acid or propanoic acid followed by an abbreviation depicting the monocarboxylic acid used (Lac=*L*-lactic acid, Prop=propanoic acid) followed by a suffix indicating which washing technique was used (not included in Scheme 1 sample names) DMF (only DMF washed) or Et₂O (DMF and Et₂O washed).

EXPERIMENTAL SECTION

Material and Synthesis. All chemicals were used

without further purification and purchased from commercial sources as follows: terephthalic acid (H₂bdc, Aldrich, 98%), zinc nitrate hexahydrate (Zn(NO₃)₂·6H₂O, Alfa Aesar, 98%), *L*-(+)-lactic acid (*L*-lac, C₃H₆O₃, Aldrich, 98%), 1-phenylethanol (1PhEtOH, C₆H₅CH(OH)CH₃, Aldrich, 98%), propanoic acid (CH₃CH₂COOH, VWR), DL- α -Hydroxy- β , β -dimethyl- γ -butyrolactone (pantolactone, C₆H₁₀O₃, Aldrich, 98%), dimethylformamide (DMF, VWR), diethyl ether ((CH₃CH₂)₂O, VWR), dichloromethane (DCM, VWR), acetonitrile (H₃CCN, VWR), dimethyl sulfoxide-d₆ (DMSO-D₆, Merck, 99.8%), conc HCl (HCl, VWR, 37 wt. %).

Synthesis of ZnBLD with a range of lactate concentration. ZnBLD was synthesized by adapting the previously reported procedure.^{2d} Briefly, zinc nitrate hexahydrate, terephthalic acid and *L*-lactic acid in varying molar quantities (Scheme 1) was dissolved in 10 mL DMF per 1 mmol zinc nitrate hexahydrate. This solution was heated in a Teflon lined stainless steel reaction vessel at 110 °C for 48 hours. After cooling to room temperature, the crystals were filtered under reduced pressure, washed with DMF and for the Et₂O washed MOFs, an additional diethyl ether wash was completed before the crystals were dried under reduced pressure.

Synthesis of ZnBLD-Propanoic acid. ZnBLD-Propanoic acid modulated MOF was prepared similarly to 0.5Lac except 0.35 mmol of propanoic acid was added to the reaction mixture before transferring to the high-pressure reactor. After adding propanoic acid, identical conditions were used for heating and crystal treatment/washing procedure. Rod-like crystals were obtained which are characteristic of the ZnBLD phase.

Characterization. FTIR spectra were recorded on a Perkin-Elmer, model Spectrum-100 a, ¹H NMR spectra were recorded on a Bruker Av500MHz solution state

Scheme 1. Compositions of the ZnBLD Synthesis.

Sample Name	Equivalence:	Equivalence:	Equivalence:	Equivalence:	Equivalence:
0.5Lac	1	0.5	130	0.5	0
0.6Lac	1	0.5	130	0.6	0
0.7Lac	1	0.5	130	0.7	0
0.8Lac	1	0.5	130	0.8	0
0.85Lac	1	0.5	130	0.85	0
0.9Lac	1	0.5	130	0.9	0
0.95Lac	1	0.5	130	0.95	0
0.35Prop	1	0.5	130	0.5	0.35

spectrometer, integrals were calculated in Mestrenova (see Figure S33 for peak characterization). PXRD traces were recorded on a PANalytical X-Pert Pro MPD X-ray diffractometer. TGA analyses were recorded on a TA Instruments TGA Q500 whilst thermogravimetric analysis-mass spectrometry (TGA-MS) traces were recorded on a Metler Toledo TGA coupled with a Hiden Analytical HPR20-QIC evolved gas mass spectrometer, both TGA and TGA-MS samples were heated in a nitrogen atmosphere at 10 °C/min from 30 °C to 900 °C. GC chromatographs were recorded on a Shimadzu 2010plus gas chromatograph fitted with an autosampler and a flame ionization detector (FID). Inductively coupled plasma measurements were recorded on a Perkin Elmer Optima 2000 DV.

¹H NMR digestion sample preparation. ¹H NMR procedure: DMSO-D₆ (0.6 mL) was added as a deuterated digestion medium to 30mg of MOF crystals, subsequently concentrated HCL was added dropwise until all the material dissolved.

Powder X-ray Diffraction measurements. MOF material (around 30 mg) was ground to a homogeneous powder in a ceramic mortar and pestle. Powder traces were recorded with 40 kV generator voltage, 20mA tube current, with Cu K α radiation at 293K. A scan step size of 0.00835 2 θ degree with a scan range from 4 to 50 2 θ degree was used. Further, the FWHM was calculated in Origin Pro using the Peaks and Baseline function (See S6).

Procedure for chiral adsorption. 0.010 g of ZnBLD was placed in a glass vial and either 0.1 mL of racemic 1-phenylethanol or 2-butanol was added or 1ml of 100mg/ml racemic pantolactone in acetonitrile. Samples were left for 24 hours at room temperature. Each sample was prepared in triplicate.

Procedure for chiral desorption. ZnBLD and the 1-phenylethanol/2-butanol/pantolactone solution was filtered under reduced pressure and lightly washed with DCM to remove residue on the surface of the crystal. After drying for a few minutes, the crystals were collected and transferred to a glass vial, 0.8 mL of DCM was added to desorb guest molecules. After 24 hours at room temperature, 0.4 mL of supernatant was taken from each vial and analyzed by chiral gas chromatography.

Chiral Gas Chromatography. All analytes were separated on a Supelco Beta Dex 120 capillary column. The conditions for 1-phenylethanol were as follows: Injection; 1 μ L split ratio of 100:1, injection port temperature: 200 °C, column isothermal at 120 °C for 28 minutes, ramped at 10 °C/min to 170 °C holding for 6 minutes (post elution of both enantiomers), FID at 210 °C, carrier gas of helium 20 cm/sec. 2-butanol; Injection; 1 μ L split ratio: 100:1, injection port temperature: 200 °C, column temperature isothermal at 30 °C for 44 minutes, ramp at 10 °C/min to 170 °C holding for 6 minutes (post elution of both enantiomers), FID at 210 °C, helium carrier gas 15 cm/sec. Pantolactone, : Injection; 1 μ L split ratio: 50:1, injection port temperature: 250 °C, column temperature isothermal at 50 °C for 5 minutes, ramp at 5 °C/min to 200 °C, FID at 210 °C, carrier gas helium 60 cm/sec.

Enantiomeric Excess (ee%). Each sample was injected three times and the standard deviation was used to calculate error bars. The separation capacity was evaluated by calculating the ee% value, comparing peak areas of each enantiomer according to Eq. (1). Where, *S* is the fraction of *S* isomer and *R* is the fraction of *R* isomer. When applied to gas chromatography, the area of each peak is used.

$$ee\% = \left(\frac{R - S}{R + S} \right) \times 100\% \quad (1)$$

RESULTS AND DISCUSSION

¹H NMR spectra were recorded and used to determine the relative concentration of *L*-lactic acid, terephthalic acid and DMF in the frameworks by integration of selected peaks (see S5 for further details). The expected ratio of 0.85:0.5 of *L*-lactic acid: terephthalic acid was not observed for 0.85Lac. Instead there was a slight increase from 0.5Lac to 0.85Lac (Figure 1a). We attributed this to missing terephthalate linkers in the framework and calculated that there were 1 in 20 missing terephthalate linkers in 0.85Lac.^{11a} 0.35Prop did not contain a higher concentration of lactic acid, as expected, instead a small amount of propanoic acid was detected for 0.35Prop, there was some

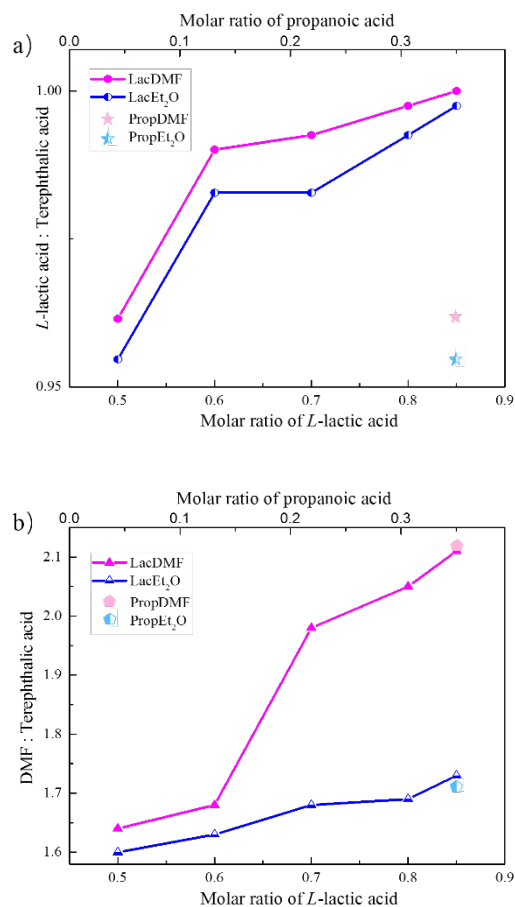


Figure 1. ¹H NMR integral data: (a) comparing peak area ratio of *L*-lactic acid: terephthalic acid with molar concentration of monocarboxylic acid, (b) comparing peak area ratio of DMF: terephthalic acid and molar ratio of monocarboxylic acid.

overlap with other peaks and therefore the propanoic acid concentration could not be determined accurately. ICP analysis also confirmed higher Zn content for the defective frameworks, (see S8 and table S1 for details). Additionally, an increase in DMF concentration was observed from 0.5Lac to 0.85Lac frameworks. As there is no difference in the MOF structure we can describe this increase in DMF as an increase in porosity of the framework as solvated guest molecules. The DMF: terephthalic acid ratio of 0.35Prop and 0.85Lac were very similar and overlap in Figure 1b indicating that the enhanced porosity was present in 0.35Prop MOFs. An increase in porosity can be expected with increasing missing linker defect concentration as the total void space increases with monocarboxylic acid replacement. Increased porosity has been correlated with missing linker defects in several studies.^{10a, 11a} Frameworks also contained varying amounts of formate, generated by DMF hydrolysis, however there was no correlation between formate concentration and *ee*% or defect concentration (See Figure S33) therefore we discounted this as insignificant.

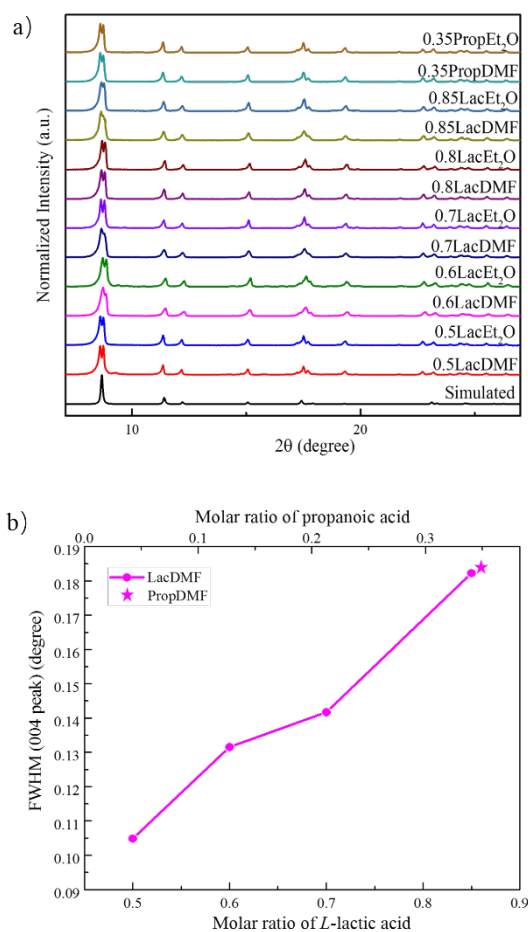


Figure 2. Powder diffraction patterns of (a) as-synthesized MOFs in this study. (b) the FWHM of (004) peak with a Gaussian shape profile fitted for 0.5–0.85LacDMF and 0.35PropDMF.

PXRD traces (Figure 2a) were highly crystalline and the increase in defect concentration did not have an effect in peak positions or relative intensities. A secondary phase could be assigned to Zn(bdc)·xH₂O (8.6 2θ degree) from

partial hydrolysis of the framework. This has been previously reported in MOF-5 PXRD traces.¹⁶ Unfortunately this peak overlapped with the 001 peak from the ZnBLD phase. In order to confirm higher defect concentrations with increasing monocarboxylic acid concentration, we compared full width at half maxima (FWHM) values. FWHM is inversely proportional to crystallite size which can be described by the Scherrer Eq. (2). Crystallite size is inversely proportional to the defect concentration in crystalline solids,¹⁷ therefore the FWHM is proportional to the defect concentration for a PXRD trace.

$$FWHM = \frac{K\lambda}{\varepsilon \cos \theta} \quad (2)$$

Where:

FWHM is in radians, *K* is the Scherrer constant (a dimensionless number near 0.9), λ is the wavelength of the radiation (in this case,), ε is the grain size (nm) and θ presents Bragg angle (in degrees).

Diffraction peaks were selected to calculate the FWHM using a Gaussian function fit profile (Peak Analyzer, OriginPro 2016) (See S6). Figure 2b shows how FWHM for the 004 peak varies with increasing molar ratio of *L*-lactic acid, 0.35PropDMF and 0.85LacDMF overlap for the 004 peak (see Figure S48 for all peak FWHM values). For all diffraction peaks, there was an increase in FWHM with increasing molar ratio of *L*-lactic acid. The increase in FWHM contributes to our overall hypothesis that the frameworks synthesized with higher concentrations of monocarboxylic acid are more defective.

TGA traces were recorded for 0.5LacDMF, 0.5LacEt₂O, 0.85LacDMF, 0.85LacEt₂O, 0.35PropDMF and 0.35PropEt₂O to investigate the thermal stability and weight losses of the various frameworks. Figure 3 shows TGA traces for 0.5LacEt₂O and 0.85LacEt₂O (See S7 for all other TGA traces recorded). The weight loss below 200°C was attributed to guest molecule removal of DMF, this confirmed higher proportions of DMF were present in the more defective MOFs. No difference in stability was observed for the defective and non-defective frameworks. Through TGA-MS experiments we did not observe monocarboxylic acid removal of lactic acid between 200 and 350°C.^{11a} As expected from ¹H NMR digestion experiments, the more defective MOFs have higher weight losses below 200°C.

For the 1-phenylethanol separation (Figure 4a), our results show a steady increase in *ee*% from 0.5Lac to 0.85Lac where we observed a plateau in *ee*%. For 1Lac, the characteristic needle like crystals of ZnBLD (See Image S1) were not obtained and there was poor adsorption of 1-phenylethanol and no enantioseparation. The largest *ee*% increase of over 35% was observed from 0.5LacDMF to 0.85LacDMF. DMF washing proved to be superior to DMF and Et₂O washing for the separation of 1-phenylethanol. The solvation of the framework plays an essential role in the success of the separation. DMF has also been shown to play a critical role for enantioseparation in two other homochiral MOF studies where the coordinated DMF carbons interact with the OH

groups of 1-phenylethano.^{8,18} Our results indicate that solvated DMF molecules can enhance the enantioseparation. For 2-butanol and pantolactone (Figure 4b, 4c) there was little to no change in *ee*% between the different washing techniques indicating that partial removal of solvated DMF did not have negative consequences for all separation processes although it appears to be a redundant step in the synthesis.

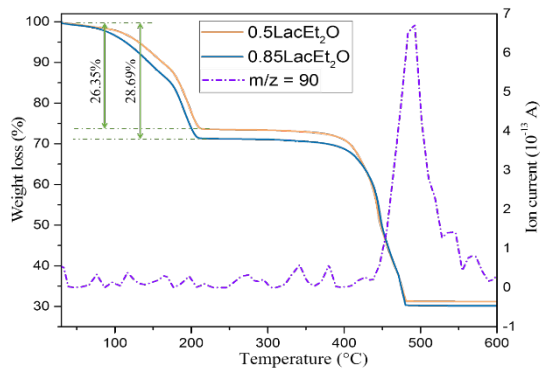


Figure 3. TGA traces (solid lines, left axis) of 0.5LacEt₂O and 0.85LacEt₂O. TGA-MS trace of 0.5LacEt₂O, dashed line, right axis.

Additionally, there was no change in the separation capacity for 2-butanol and pantolactone between the non-defective and defective frameworks. We rationalise that the selectivity increases for 1-phenylethanol, the largest molecule we separated because the introduction of missing linker defects increases the pore size for some pores and allows for enhanced separation capacities due to a subtle change in host-guest interactions (See S9 for calculated area of all test molecules).

Figure 5 shows the correlation between DMF concentration and *ee*% for 1-phenylethanol. There is a clear trend between DMF concentration and *ee*% for both DMF and Et₂O washed frameworks. The 0.35Prop MOFs also follow the trend for both washing techniques. This highlights the correlation between framework porosity and separation capacity.

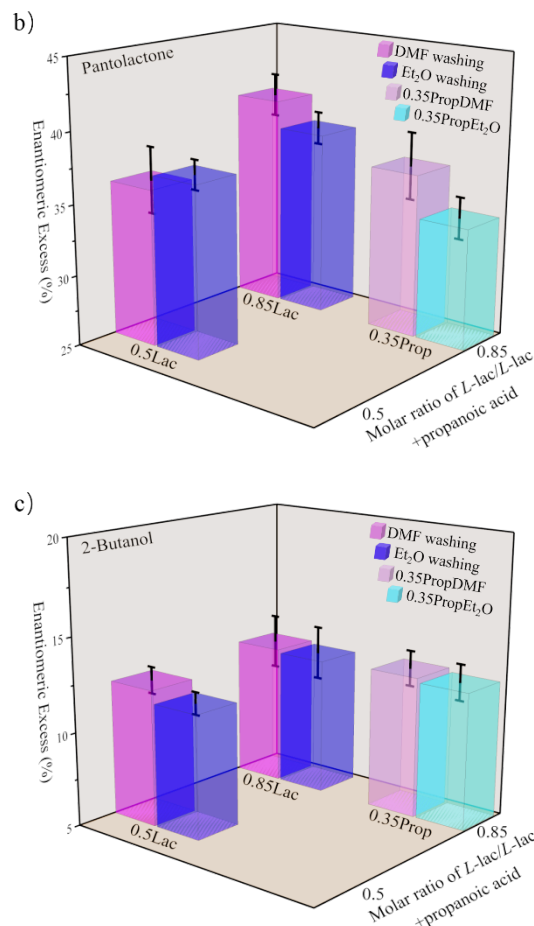
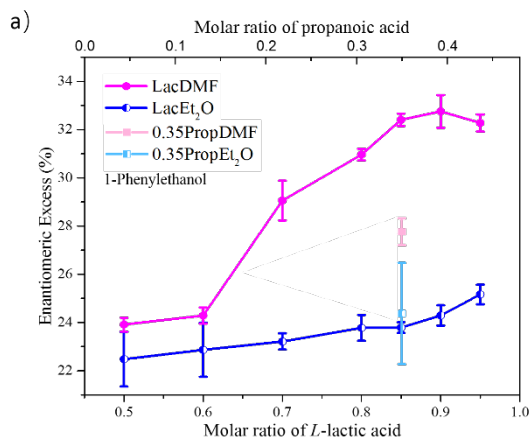


Figure 4. Enantioselective capacity: (a) 1-phenylethanol sorption for 0.5Lac to 0.95Lac and 0.35Prop: enhancement in *ee*% value as a function of increasing monocarboxylic acid concentration with different washing techniques. (b) 2-butanol sorption experiment for the 0.5Lac, 0.85Lac and 0.35Prop series. (c) pantolactone sorption experiment for the 0.5Lac, 0.85Lac and 0.35Prop series.

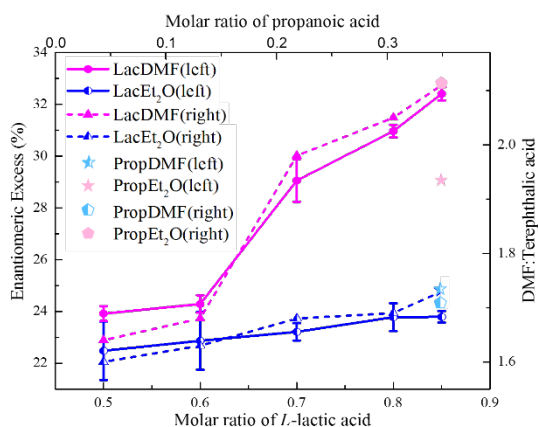


Figure 5. An overlay of Figures 1b and 4a, showing the correlation between DMF concentration (from ¹H NMR digestion data) of the monocarboxylic acid modulated frameworks and enantiomeric excess for 1-phenylethanol.

CONCLUSIONS

In summary, we have shown for the first time how the enantioselective properties of a MOF can be enhanced by introducing missing linker defects. An increase in enantiomeric separation was observed with increasing defect concentration for 1-phenylethanol. No increase in separation was observed for 2-butanol or pantolactone. ¹H NMR digestion data supports missing terephthalate linker defects and as expected this gives a slightly higher porosity (higher DMF: terephthalic acid ratio), a higher proportion of DMF is also observed in TGA traces for the more defective MOFs. We cannot conclude that a higher porosity is responsible for an increase in enantiomeric excess. Instead we describe the increased enantioselectivity as being caused by a larger pore size which provides a better fit for the guest molecules of 1-phenylethanol, the smaller guest molecules of 2-butanol and pantolactone do not benefit from the enhanced separation due to the smaller molecular area of these molecules. We hope that implications of our results significantly decrease the costs involved for industrial applications of these materials, by partially replacing expensive enantiopure ligands with cheap alternatives such as propanoic acid.

ASSOCIATED CONTENT

Supporting Information. Additional method details, microscope crystal image, GC chromatograms, FTIR spectra, Calculation details for NMR spectra, methods for the calculation of FWHM from PXRD, TGA traces, ICP analysis details and molecular area of test molecules are available in the supporting information. This material is available free of charge via the Internet at <http://pubs.acs.org>.

AUTHOR INFORMATION

Corresponding Author

*Bradley P. Ladewig b.ladewig@imperial.ac.uk

Author Contributions

[§]BS and ZW contributed equally to this work

ACKNOWLEDGMENT

BS acknowledges The Commonwealth Scientific and Industrial Research Organization and Imperial College London for financial support. ZW acknowledges the China Scholarship Council for financial support. Dr Lisa Haigh and Peter Haycock are acknowledged for their assistance with mass spectrometry and NMR spectroscopy respectively. Additionally, We would like to thank Diamond Light Source for access to B23 (CM16778) and Prof Giuliano Siligardi and Dr Rohanah Hussain for their time and effort measuring and analysing circular dichroism spectra.

REFERENCES

- (1) Chankvetadze, B.; Chankvetadze, L.; Sidamonidze, S.; Yashima, E.; Okamoto, Y. *J. Pharm. Biomed. Anal.* **1996**, *14*, 1295.
- (2) (a) Zhang, J.; Li, Z.; Gong, W.; Han, X.; Liu, Y.; Cui, Y. *Inorg. Chem.* **2016**, *55*, 7229 (b) Zhang, S.-Y.; Wojtas, L.; Zaworotko, M. J. *J. Am. Chem. Soc.* **2015**, *137*, 12045 (c) Chang, C. L.; Qi, X. Y.; Zhang, J. W.; Qiu, Y. M.; Li, X. J.; Wang, X.; Bai, Y.; Sun, J. L.; Liu, H. W.

- Chem. Commun.* **2015**, *51*, 3566 (d) Dybtsev, D. N.; Nuzhdin, A. L.; Chun, H.; Bryliakov, K. P.; Talsi, E. P.; Fedin, V. P.; Kim, K. *Angew. Chem. Int. Ed.* **2006**, *45*, 916 (e) Gu, Z. G.; Grosjean, S.; Bräse, S.; Wöll, C.; Heinke, L. *Chem. Commun.* **2015**, *51*, 8998.
- (3) (a) Lee, J.; Farha, O. K.; Roberts, J.; Scheidt, K. A.; Nguyen, S. T.; Hupp, J. T. *Chem. Soc. Rev.* **2009**, *38*, 1450 (b) Gole, B.; Sanyal, U.; Banerjee, R.; Mukherjee, P. S. *Inorg. Chem.* **2016**, *55*, 2345 (c) Luque, R.; Li, Y. *Chemical Science* **2014**, *5*, 3708 (d) Nuzhdin, A. L.; Dybtsev, D. N.; Bryliakov, K. P.; Talsi, E. P.; Fedin, V. P. *J. Am. Chem. Soc.* **2007**, *129*, 12958.
 - (4) (a) Zheng, H.; Zhang, Y.; Liu, L.; Wan, W.; Guo, P.; Nyström, A. M.; Zou, X. *J. Am. Chem. Soc.* **2016**, *138*, 962 (b) Ray Chowdhuri, A.; Bhattacharya, D.; Sahu, S. K. *Dalton Trans* **2016**, *45*, 2963.
 - (5) (a) Spanopoulos, I.; Tsangarakis, C.; Klontzas, E.; Tylianakis, E.; Froudakis, G.; Adil, K.; Belmabkhout, Y.; Eddaoudi, M.; Trikalitis, P. N. *J. Am. Chem. Soc.* **2016**, *138*, 1568 (b) Zhang, M.; Li, B.; Li, Y.; Wang, Q.; Zhang, W.; Chen, B.; Li, S.; Pan, Y.; You, X.; Bai, J. *Chem. Commun.* **2016**, *52*, 7241.
 - (6) Xu, Z. X.; Fu, H. R.; Wu, X.; Kang, Y.; Zhang, J. *Chem. Eur. J.* **2015**, *21*, 10236.
 - (7) Li, P.; He, Y.; Guang, J.; Weng, L.; Zhao, J. C. G.; Xiang, S.; Chen, B. *J. Am. Chem. Soc.* **2014**, *136*, 547.
 - (8) Suh, K.; Yutkin, M. P.; Dybtsev, D. N.; Fedin, V. P.; Kim, K. *Chem. Commun.* **2012**, *48*, 513.
 - (9) (a) Fang, Z.; Bueken, B.; De Vos, D. E.; Fischer, R. A. *Angew. Chem. Int. Ed.* **2015**, *54*, 7234 (b) Sholl, D. S.; Lively, R. P. *J. Phys. Chem. Lett.* **2015**, *6*, 3437.
 - (10) (a) Wu, H.; Chua, Y. S.; Krungleviciute, V.; Tyagi, M.; Chen, P.; Yildirim, T.; Zhou, W. *J. Am. Chem. Soc.* **2013**, *135*, 10525 (b) Gutov, O. V.; Hevia, M. G.; Escudero-Adán, E. C.; Shafir, A. *Inorg. Chem.* **2015**, *54*, 8396 (c) Van de Voorde, B.; Stassen, I.; Bueken, B.; Vermoortele, F.; De Vos, D.; Ameloot, R.; Tan, J.-C.; Bennett, T. D. *J. Mater. Chem. A* **2015**, *3*, 1737.
 - (11) (a) Shearer, G. C.; Chavan, S.; Bordiga, S.; Svelle, S.; Olsbye, U.; Lillerud, K. P. *Chem. Mater.* **2016**, *28*, 3749 (b) Schaate, A.; Roy, P.; Godt, A.; Lippke, J.; Waltz, F.; Wiebcke, M.; Behrens, P. *Chem. Eur. J.* **2011**, *17*, 6643 (c) Tsuruoka, T.; Furukawa, S.; Takashima, Y.; Yoshida, K.; Isoda, S.; Kitagawa, S. *Angew. Chem. Int. Ed.* **2009**, *48*, 4739 (d) Cliffe, M. J.; Castillo-Martínez, E.; Wu, Y.; Lee, J.; Forse, A. C.; Firth, F. C. N.; Moghadam, P. Z.; Fairen-Jimenez, D.; Gaultois, M. W.; Hill, J. A.; Magdysyuk, O. V.; Slater, B.; Goodwin, A. L.; Grey, C. P. *J. Am. Chem. Soc.* **2017**, *139*, 5397.
 - (12) Hu, Z.; Peng, Y.; Kang, Z.; Qian, Y.; Zhao, D. *Inorg. Chem.* **2015**, *54*, 4862.
 - (13) Vermoortele, F.; Bueken, B.; Le Bars, G.; Van de Voorde, B.; Vandichel, M.; Houthoofd, K.; Vimont, A.; Daturi, M.; Waroquier, M.; Van Speybroeck, V.; Kirschhock, C.; De Vos, D. E. *J. Am. Chem. Soc.* **2013**, *135*, 11465.
 - (14) Cliffe, M. J.; Hill, J. A.; Murray, C. A.; Coudert, F.-X.; Goodwin, A. L. *Phys. Chem. Chem. Phys.* **2015**, *17*, 11586.
 - (15) Navarro-Sánchez, J.; Argente-García, A. I.; Moliner-Martínez, Y.; Roca-Sanjuán, D.; Antypov, D.; Campíns-Falcó, P.; Rosseinsky, M. J.; Martí-Gastaldo, C. *J. Am. Chem. Soc.* **2017**, *139*, 4294.
 - (16) Ravon, U.; Savonnet, M.; Aguado, S.; Domine, M. E.; Janneau, E.; Farrusseng, D. *Microporous Mesoporous Mater.* **2010**, *129*, 319.
 - (17) Baig, A. A.; Fox, J. L.; Young, R. A.; Wang, Z.; Hsu, J.; Higuchi, W. I.; Chhetry, A.; Zhuang, H.; Otsuka, M. *Calcif. Tissue Int.* **1999**, *64*, 437.
 - (18) Dybtsev, D. N.; Yutkin, M. P.; Samsonenko, D. G.; Fedin, V. P.; Nuzhdin, A. L.; Bezrukov, A. A.; Bryliakov, K. P.; Talsi, E. P.; Belosludov, R. V.; Mizuseki, H.; Kawazoe, Y.; Subbotin, O. S.; Belosludov, V. R. *Chem. Eur. J.* **2010**, *16*, 10348.

